

Moisture and temperature balances  
at the ARM Southern Great Plains Site  
in forecasts with the CAM2

D. L. Williamson<sup>1</sup>, J. Boyle<sup>2</sup>, R. Cederwall<sup>2</sup>, M. Fiorino<sup>2</sup>,  
J. Hnilo<sup>2</sup>, J. Olson<sup>1</sup>, T. Phillips<sup>2</sup>, G. Potter<sup>2</sup> and S. C. Xie<sup>2</sup>

<sup>1</sup>National Center for Atmospheric Research, Boulder, Colorado

<sup>2</sup>Lawrence Livermore National Laboratory, Livermore, California

Submitted to *Journal of Geophysical Research*

8 june 2004

Corresponding author's address:

David L. Williamson

National Center for Atmospheric Research

Box 3000

Boulder, CO 80307-3000

e-mail: [wmson@ucar.edu](mailto:wmson@ucar.edu)

## ABSTRACT

We compare the balance of terms in the moisture and temperature prediction equations during short forecasts by the Community Atmosphere Model (CAM2) with observed estimates at the ARM Southern Great Plains site for two IOPs. The goal is to provide insight into parameterization errors which ultimately should lead to model improvements. The atmospheric initial conditions are obtained from high resolution NWP analyses. The land initial conditions are spun up to be consistent with those analyses. Three cases are considered: (1) June/July 1997 when the atmosphere is relatively moist and surface evaporation corresponds to 90% of the precipitation with advection accounting for the remainder; (2) rainy days in April 1997 when the atmosphere is less moist and horizontal advection accounts for much of the precipitation with a small contribution from surface evaporation and the balance being derived from the water already present in the column, and (3) non-rainy days of the April 1997 when the moist process parameterizations are inactive and the PBL parameterization is dominant. For the first case the Zhang-McFarlane convective parameterization drives the model to a wrong state. For the second, the Hack convective parameterization appears to be not acting deep enough. During both periods inconsistencies between CAM2 and ARM surface fluxes, land surface conditions, and the net surface radiative fluxes indicate that the exchange parameterizations should be examined further. For the third case, the PBL parameterization does not appear to create the correct vertical structure. In addition, the individual components of the dynamical tendency are very different between CAM2 and ARM, although the total dynamical tendency is similar in the two. Although these observations do not imply that those components are themselves wrong since they may be responding to other errors, each of these components should be examined further to determine the cause of their behaviors.

## 1. Introduction

We compare the balance of terms in the moisture and temperature prediction equations during short forecasts from a climate model with observed estimates at the U. S. Department of Energy (DOE) Atmospheric Radiation Measurement (ARM) Program's Southern Great Plains site for two Intensive Observing Periods (IOPs.) The approach compares parameterized variables from subgrid-scale parameterizations applied to the true atmospheric state with atmospheric analyses and field campaign data such as those from ARM. The goal is to provide insight into parameterization errors which ultimately should lead to model improvements. Our effort has been designated the CCPP-ARM Parameterization Testbed (CAPT) where CCPP is the DOE Climate Change Prediction Program. Phillips et al. (2004) provide an overview of our methods. This forecast approach is used routinely and very successfully at Numerical Weather Prediction (NWP) centers as part of their model development activities. The primary difference between their application and ours is one of scale. The NWP models are applied at very high resolution in order to predict the detailed evolution of the weather. The climate models such as ours are applied at modest resolution and more scales must be addressed by the parameterizations. Our forecasts are made at the climate model application resolution since that is the resolution for which we wish to gain improved parameterizations.

We examine forecasts with the Community Atmosphere Model Version 2 (CAM2) coupled to the Community Land Model (CLM2). The CAM2 is the successor to the Com-

munity Climate Model (CCM3) (Kiehl et al. 1998). Kiehl and Gent (2004) summarize the improvements to the physical parameterizations in CAM2 over the those in CCM3. More complete documentation can be found at <http://www.cesm.ucar.edu/models/atm-cam/> which includes a technical description of the algorithms in the model. Our forecasts are made at the standard CAM2 development and application resolution: T42 spectral truncation on a  $64 \times 128$  point latitude-longitude Gaussian grid and 26 vertical levels. Bonan et al. (2002) provide details of the improvements provided by CLM2 over the previous land model LSM which was coupled to CCM3. Additional information on CLM2 can be found at <http://www.cgd.ucar.edu/tss/clm/>.

The initial atmospheric conditions are obtained by mapping high resolution NWP analyses to the coarse resolution climate model grid in a way that is consistent with the low resolution topography, and leads to smooth, balanced forecasts. We follow the method described in White (2001). For most of the forecasts discussed here the initial conditions are from the ECMWF reanalyses (ERA40) described by Simmons and Gibson (2000). We have performed matching forecasts from the NCEP-DOE reanalyses (R2) described by Kanamitsu et al. (2002) to determine the sensitivity of our results to the initial analyses. In general, the errors we consider are very similar in forecasts initialized from the two analyses. Forecasts from analyses from several NWP centers are useful to indicate sensitivity to the initial analyses. If only minimal sensitivity is found one has more confidence that the model is being compared to the atmosphere. With strong sensitivity there is the danger that each NWP analysis is dominated by its native model and that one

is just comparing one's model to the NWP models. We concentrate on forecasts from the ERA40 data and occasionally point out differences from forecasts from the R2 data. The land initial conditions are obtained by a spinup procedure in which the CLM2 responds to and interacts with the CAM2 while the CAM2 is forced with NWP analyses to evolve like the observed atmosphere. This is described in more detail in Phillips et al. (2004) and Boyle et al. (2004). Some indication of the quality of the land initial conditions is provided in Boyle et al. (2004) and will be summarized later with regard to their potential influence on the behavior of the parameterizations.

In this study the balance of terms in the CAM2 forecasts is verified using the ARM IOP data sets that were developed for forcing and diagnosing single column and cloud resolving models. These have been processed with the constrained variational analysis method of Zhang and Lin (1997) and Zhang et al. (2001). These data include the variables needed to drive single column models and additional fields for diagnostic purposes such as the surface radiation measurements from the network of SIROS stations. These data also include estimates of the sub-grid scale forcing equivalent to what would be calculated by a model parameterization suite. These are obtained as a residual of the total tendency minus the advective or dynamical terms. We often refer to these as the ARM parameterizations, but, of course, they are not calculated as such. More details in addition to those in the cited papers can be found at <http://www.arm.gov/docs/scm/variational/>. We refer to these as the ARM data. Although there are uncertainties in these data, as in any data set based on observations, they do expose what appear to be rather gross, first-order model

errors. The uncertainties in the variational data set become more problematical for more subtle model errors. Nevertheless, comparison of the model forecasts with them does seem to provide an indication of which model components warrant further examination with perhaps additional datasets.

The CAM2 forecasts are initialized every day at 00Z for the ARM IOPs considered. The forecast data are archived every three hours; instantaneous values for state variables such as temperature and specific humidity, and 3-hr averages for forcing terms such as parameterized heating and moistening rates. For much of our analysis these heating and moistening rates are further averaged to 12- or 24-hour averages. The ARM data are averaged the same way.

The CAM2 data are the average over the four CAM2 grid boxes surrounding the ARM SGP site. Although the area of the ARM region was chosen to be comparable to the area of a single typical climate model grid box, the ARM central site does not coincide with the center of a CAM2 grid box. Rather the site falls very near the vertices of four CAM2 grid boxes. Boyle et al. (2004) illustrate this overlap. Thus the area represented by the CAM2 data is at least twice as large as that of the ARM data. We comment further on this where it affects the comparisons.

We will consider both the set of individual forecasts at fixed elapsed times and the ensemble or composite averages of forecasts. The average of forecasts will be referred to as the mean forecast. The composites are chosen to consist of forecasts with like errors. The individual forecasts are used to determine the members for the composite averages.

We concentrate on mean forecasts to better uncover systematic errors. Single forecast errors might be unique and thus less useful in establishing general model behavior. Single representative forecasts, however, are likely to be useful for more detailed examination of model changes in future studies.

We will use the term “CAM2 error” to refer to CAM2 minus ARM differences. One should keep in mind that this difference includes the CAM2 error itself, which is usually assumed to be the dominant component, and errors in the ARM measurements and variational analysis, as well as differences due to the CAM2 and ARM data representing different areas. It is practically impossible to differentiate between all these sources of differences, especially as error bars for the ARM data are not known.

Of course budget studies such as we analyse here illustrate the “chicken and egg” problem; the true cause and effect is difficult to untangle. Nevertheless, they do indicate which processes are going wrong first and thus areas that could probably benefit from further consideration.

Phillips et al. (2004) show via the 500mb anomaly correlation skill score that the CAM2 makes credible forecasts of the large scale atmospheric state on the time scale of a few days. These scores indicate that at least the forecast patterns are consistent with the atmosphere and thus the large scale forcing of the parameterizations involve the correct phenomena. However, we will see that in some cases significant errors develop rapidly in some state variables such as temperature and moisture. Boyle et al. (2004) provide a synoptic view for a single not atypical forecast over continental US. This also illustrates

that in the first few days of the forecasts the large scale state variables driving the CAM2 parameterizations are reasonably close to the atmosphere. Thus further detailed examination of the parameterized processes in such forecasts is warranted.

In Section 2 we consider the forecasts for the June/July 1997 IOP and in Section 3 we consider the forecasts for the April 1997 IOP. The latter set is divided into those for days when it rained and those when there was little or no rain. The data examined represent the vertical atmosphere column at the ARM site. Finally, in Section 4 we summarize our conclusions.

## 2. June/July 1997 IOP Forecasts

Fig. 1 shows the vertical profiles of the mean forecast temperature and specific humidity errors as a function of forecast time for five day forecasts. There is a modest error at  $t = 0$  due to the difference between the ERA40 analyses interpolated to the CAM2 grid used as initial conditions and the ARM data. The ARM soundings are not assimilated in the ERA40. This initial warm bias has a maximum of almost 1K at 300mb. The CAM2 forecast error forms rapidly within the first 24 hours with relatively little change in the following four days except near the surface where the error decreases by a factor of 2. After 24 hours the CAM2 is too moist above 500mb and in the surface layers, and too dry between 900mb and 500mb. The CAM2 becomes too warm between 900mb and 200mb and too cold below that region. The CAM2 is too cold above that region initially and remains that way.

As mentioned above, it is useful to consider forecasts initialized with analyses pro-

duced by several NWP centers to determine what aspects of the model behavior are robust and not dependent on a particular analysis, assuming all analyses used are reasonable representations of the atmosphere. To save space we do not show similar plots of the forecasts from the R2 analyses, but rather describe the differences from those in Fig. 1. The initial temperature error for the mean forecast from the R2 analyses interpolated to the CAM2 grid is slightly less than that from the ERA40 analyses. It reaches a maximum of 0.6K at 300mb instead of 1K. The specific humidity however has a larger initial error of -1.75 g/kg at the surface decreasing to zero at 800mb. This difference has a modest effect on the mean forecast temperature error at day 1. The error is 2K from 500mb to 200mb, rather than continuing to increase above 500mb as seen in Fig. 1. The temperature error at 900mb is double that seen in Fig. 1. The specific humidity error is similar in the two sets of forecasts. In the following we will first consider the ERA40 forecasts and later discuss the ramifications of the different initial analyses on the forecasts.

Fig. 1 shows the error in the mean forecast. In fact virtually every forecast comprising the mean shows similar errors. Fig. 9 of Boyle et al. (2004) shows the 24-hour relative humidity errors for the individual forecasts. Although the atmosphere experiences periods that are relatively moist or dry, the CAM2 forecasts invariably become very moist in the upper troposphere with relative humidities of 70% to 90%. The mid to lower troposphere tends to dry in the forecasts and the lowest model levels become too moist. The ARM data indicate that the maximum relative humidity is centered at 850mb and extends from 900mb to 750mb. After 24 hours the CAM2 forecasts have the maximum relative humid-

ity values restricted to the lowest model level around 950mb. This systematic behavior justifies studying the mean forecast for the entire IOP in Fig. 1 above and in the following.

Since the CAM2 forecast errors form rapidly within 24 hours, we consider the terms in the moisture equation averaged over the first 24 hours of the forecasts. In addition, we consider only the mean forecast error rather than the errors of individual forecasts. Figure 2 shows vertical profiles of the 24-hour average of terms in the specific humidity tendency equation for the mean CAM2 forecast and the corresponding ARM data. The specific humidity equation can be written

$$\frac{\partial q}{\partial t} = -\mathbf{V} \cdot \nabla q - \dot{\sigma} \frac{\partial q}{\partial \sigma} + S \quad (1)$$

where the source term  $S$  represents the sub-grid scale parameterizations. The first two terms on the right-hand-side denote the horizontal and vertical advection. We also consider the sum of these two – the total advection. For the CAM2 we separate the source term into two primary components referred to as the moist processes parameterization and the planetary boundary layer (PBL) parameterization. The PBL parameterization includes the surface fluxes which are distributed in the vertical by the PBL parameterization (Holtslag and Boville, 1993). The moist processes include both the Zhang and McFarlane (1995) and Hack (1994) convection parameterizations and the prognostic cloud water parameterization (Rasch and Kristjansson, 1998). Each of these moist components has a complementary term which evaporates falling rain water created by that component. We refer to these as rainfall evaporation. Roads et al. (1998) performed a similar budget analysis for NCEP model forecasts averaged over the Mississippi River basin. However,

they averaged over full seasons and did not have corresponding verification data such as the ARM data used here.

We consider first the budget terms from the ARM data in Fig. 2a which shows the total tendency (left-hand side of Eq. 1) and the contributions to the total from the advection and from the parameterizations. The observed total moisture tendency in ARM (dashed blue) is near zero. This is created by a balance of the advection and parameterizations. The advection (dashed red) decreases the moisture below 800mb and increases it above. Fig. 2c shows that the ARM horizontal advection (dashed blue) is negative throughout the column and the vertical (dashed green) is positive above 850mb and near zero below. The vertical advection is slightly larger than the horizontal yielding the total advection source above 800mb, which is balanced by removal by the parameterizations (dashed green, Fig. 2a.) Below 850mb the parameterizations are a source which presumably is due to surface evaporation distributed vertically by the PBL.

The total moisture tendency in CAM2 (solid blue, Fig. 2a) shows very large negative values centered at 850mb with smaller positive values above 500mb. In CAM2 the parameterizations (solid green) dominate the total tendency. The CAM2 advection (solid red) is similar to that of ARM, but slightly larger below 600mb, perhaps a result of the CAM2 moisture already departing from the observed values in the 24-hour period of the average.

Fig. 2b shows the components of the total parameterized source for CAM2. A similar partition is, of course, unavailable from ARM. The moist processes (red) dominate the total (green) above 850mb where the PBL parameterization (blue) goes to zero. The moist

processes are further divided into the individual components in Fig. 2d. The dominant component responsible for the drying is the Zhang-McFarlane convective parameterization (solid blue). The rainfall evaporation accompanying the Zhang-McFarlane parameterization (dashed blue) moistens throughout the column and contributes to much of the moistening above 500mb. The Hack convective and prognostic cloud parameterizations and their rainfall evaporations add a minor contribution to the moistening above 500mb. Boyle et al. (2004) point out that a large contribution to the model error is introduced between 09LST and 15LST, consistent with convective origins. Since the Zhang-McFarlane convection is the dominant component, it is reasonable to assume that this parameterization is driving the model to the wrong state. Of course this does not necessarily imply that the convection parameterization itself is incorrect. It might be responding to incorrect forcing from some other term such as the surface flux/PBL parameterization. On the other hand, perhaps one of the other moist process components should be more active. In fact, near the surface, the total parameterized source is a balance between the convection and PBL parameterizations, and is significantly larger than the total diagnosed from the ARM data which is almost zero (green curves, Fig. 2a). Fig. 14 of Boyle et al. (2004) shows that the CAM2 PBL is too shallow by a large factor, implying that the PBL parameterization is not mixing deep enough. The PBL moistening near the surface is quite likely too large since the CAM2 latent heat flux is larger than that in the ARM data by almost  $40 \text{ W/m}^2$  (Table 1). At the same time the CAM2 sensible heat flux is smaller than that of ARM by almost  $20 \text{ W/m}^2$ . The CAM2 net radiation at the surface is in good agreement with ARM (within  $1 \text{ W/m}^2$ ) (Table 1). The different partition in CAM2 between latent

and sensible heat fluxes is probably responsible for CAM2 being too cold and too moist near the surface after one day (Fig. 1). Since the model becomes too cold and too moist near the surface after 24 hours, one would expect the sensible heat flux to increase and the latent heat flux to decrease during the second 24 hour period of the forecast, all other properties being constant. That is indeed what happens (the latent heat flux decreases by around  $15 \text{ W/m}^2$  and the sensible increases by around  $10 \text{ W/m}^2$ ) and the temperature and specific humidity differences at the first model level on day two are half those of day one, while the ARM values remain nearly the same as day one (Fig. 1). Xie et al. (2004) show that the partitioning of the surface fluxes changes when the convection scheme produces more realistic clouds and rain.

It is difficult to verify the initial soil moisture and temperature used for the forecasts. Boyle et al. (2004) discuss this issue and attempt to determine at least the relative accuracy of the land initial conditions. They conclude that the CLM2 land initial conditions are reasonably good, but if anything the land is too warm and too dry. On the other hand, we saw above that the latent heat flux is too large and the sensible heat flux is too small during the first 24 hours of the forecast. Thus the land initial conditions appear not to be responsible for the incorrect partition between latent and sensible heat fluxes in the CAM2 forecasts, and the exchange parameterizations should be examined further.

Table 1 shows that the net long and short wave surface fluxes both agree well with the ARM estimates. The differences between CAM2 and ARM are less than  $15 \text{ W/m}^2$  and probably within the observational uncertainty and/or are associated with areal differences

between the effective CAM2 and ARM spatial domains. More notable is the difference in cloud fraction. Both the low cloud and high cloud fractions are significantly overestimated in CAM2 (Table 1). The cloud liquid water is also overestimated in the CAM2 (Table 1). However the ARM value might be an underestimate during periods of heavy rain (J. J. Yio, personal communication). This seeming contradiction between cloud water and net solar surface flux arises because the values in the figure are 24-hour averages, and it is partly explained by considering the diurnal cycle of the mean forecast. The cloud liquid water has a maximum (of 3-hour averages) for the period from 12Z–15Z (06LST–09LST). The maximum in CAM2 is twice that of ARM, but the minimum value in CAM2 which occurs for the three hour period 21Z–24Z (15LST–18LST) is close to that of ARM. Thus, much of the difference occurs at night, although the daylight average differences are not exactly zero.

The cloud fraction properties of CAM2 however remain quite different from those of ARM when the diurnal cycle is considered (not shown). The CAM2 low and mid-level cloud fractions are almost 180 degrees out of phase with ARM. The CAM2 high cloud fraction is 180 degrees out of phase with CAM2 low cloud fraction, but the ARM high cloud fraction (sampled to correspond to the mean forecast) is nearly constant. It is not clear that cloud fraction represents the same quantity in the CAM2 and ARM data sets and we do not consider it further here. The cloud fractions should be calculated with a forward model in CAM2 to represent the same variables that are provided by ARM. In addition, Boyle et al. (2004) point out that the somewhat traditional division into

low, middle and high categories, in this case at least, mixes together different types of errors, and thus is less suitable for diagnosing the behavior of the parameterizations than considering more detailed vertical structure.

As was noted earlier, the CAM2 forecasts invariably become very moist in the upper troposphere while the ARM data show more variation from day to day. This difference in variability is also seen in the 24-hour average precipitation for the individual forecasts shown in Fig. 3a. There is much less variation from day to day in CAM2 which tends to rain every day with the amounts only marginally related to the ARM values. The ARM precipitation is much more episodic showing days with intense rain separated by days with no or very little rain. Boyle et al. (2004) compare the precipitation from these forecasts in more detail with additional observations and consider the effect of averaging over four grid cells in the CAM2 analysis. They conclude that the different averaging domains do not account for the different precipitation frequency. The rain in CAM2 during June/July 1997 is almost entirely convective, arising from the Zhang-McFarlane parameterization. (The rain from the Hack parameterization and from the prognostic cloud component is essentially negligible.) The same precipitation characteristics are seen in runs with the single column version of CCM3 (also with the Zhang-McFarlane parameterization) when forced with observed atmospheric forcing from the same IOP as considered here (Xie et al, 2002). The moisture source balancing the precipitation in ARM is surface evaporation which is 90% of the precipitation. The advection accounts for the remainder. In CAM2 the evaporation is only 70% of the precipitation, yet as seen above (Table 1) when discussing

the latent heat flux, it is larger than that of ARM. Most of the remainder of the moisture converted into rain in CAM2 is from the atmosphere reservoir in the column.

The CAM2 does not maintain the precipitable water in its atmosphere (Fig. 3b). The amount in the mean forecast drops from 36mm initially to around 33mm after 24 hours to slightly less than 32mm after 48 hours. Fig. 3b also shows the precipitable water from the CAM2 forecasts initialized with the R2 analyses. The R2 initial precipitable water is significantly less than that of ERA40 which agrees well with the ARM estimates. This, of course, is entirely consistent with the initial specific humidity discussed with Fig. 1. After 1 day the difference in precipitable water between the ERA40 and R2 initialized mean forecasts is much reduced. Overall, there is less moisture in the R2 analyses available to drive the convection during the first day of the forecasts. Thus the mean forecast temperature error in the upper troposphere at day 1 is less with the R2 initial data than with the ERA40, as was discussed in conjunction with Fig. 1. Overall, examination of the moisture budget in the forecasts with R2 initial data shows much the same behavior as that discussed above with the ERA40 initialized forecasts. The difference is that the convective parameterization is slightly weaker. Thus the conclusions from the ERA40 initialized forecasts are robust.

There have been various studies concerning the triggering functions for the Zhang-McFarlane convection parameterization (Xie and Zhang, 2000, Xie et al. 2004) attempting to address the precipitation frequency error. However that is only one aspect of the CAM2 deficiency. Work is also needed to improve the atmospheric state created by the param-

eterization when invoked, both in terms of the total precipitable water and its vertical distribution. As mentioned above, although the Zhang-McFarlane parameterization might not be in error, it seems a good starting point to examine why it is behaving this way.

### 3. April 1997 IOP Forecasts

The behavior of CAM2 forecasts in April is very different from that in June/July. Fig. 4a shows the 24-hour average precipitation rate for the individual forecasts. In contrast to the summer case in Fig. 3a, in April the CAM2 captures the episodic nature of the precipitation observed in ARM very well. The prognostic cloud parameterization provides about one-third of the total precipitation and the convective parameterization two-thirds, almost entirely from the Hack parameterization. Fig. 4b shows that in the mean forecast the model maintains the precipitable water well during the five-day forecasts unlike the rapid decrease seen in Fig. 3b for the summer forecasts.

On the rainy days in Fig. 4a, the precipitation rate in the CAM2 forecast is about two-thirds that of the observed, but the CAM2 data, being an average of the four grid boxes surrounding the ARM region, represent a larger area. Although the area of the ARM region is comparable to a single CAM2 grid box, Fig. 1 of Boyle et al. (2004) shows that the center of the ARM region falls very near the vertices of four CAM2 grid boxes, thus no CAM2 box coincides with the ARM region. Examination of the precipitation in the four individual CAM2 grid boxes surrounding the ARM central site shows that a single grid box can capture the magnitude of each event, but no single box captures them all. The southeast box captures the first event, the northwest box captures the second

and the northeast captures the third.

The terms in the moisture and temperature prediction equations are very different on rain and no rain days. Therefore, for further analysis of the April forecasts we consider composites of days with significant precipitation (initialized Julian days 94, 98, 101) and days with zero or minimal precipitation (initialized Julian days 104-110). We refer to the latter as the no rain day composite even though it includes a few days with light rain. We consider first the composite of precipitation events.

**Composite rain case.** In an attempt to eliminate the area discrepancy between the CAM2 and ARM averages that affects the magnitudes of the parameterization terms and the comparison with ARM, we create the composite over the single grid boxes whose precipitation matches the ARM precipitation on each day. Thus, a different grid box is used for each member of the composite average. We have also considered the four-grid-box average composite and will comment on how it differs from the detailed results presented here. We perform this single grid-box composite to be able to compare like processes between the observations and the CAM2, recognizing, however, that the model may be invoking the processes in the wrong place. Fig. 4c shows the 24-hour average precipitation rate for the individual forecasts with the values verifying on days 95, 99, and 102 replaced by their selected single grid-box averages. As stated above, the model matches the ARM values rather well, although not exactly, CAM2 being about 3 mm/day less than ARM. Fig. 4d shows the evolution of the composite average precipitable water for the three forecasts. The precipitable water increases in CAM2 in the first 24 hours of

the forecasts, then decreases for the second 24-hour period, while in ARM the precipitable water decreases during the first 48 hours as the precipitation removes water from the column.

Fig. 5 shows the vertical profiles of temperature and specific humidity at zero (blue) and 24 hours (red) for the composite average CAM2 forecast (solid) and verifying ARM data (dashed). The temperature profiles are shown with a standard atmosphere (Hess, 1959, pps 84-85) removed to enlarge the scale and better show the magnitude of the differences. Once again, the CAM2 and ARM values are not the same initially (blue curves), indicating some uncertainty in the data sets. The ARM data (dashed curves) indicate cooling during the 24-hour forecast below 350mb. The CAM2 (solid curves) warms slightly between 700mb and 800mb and does not cool enough above and below. By day 1 the CAM2 thus is too warm compared to ARM (red curves), with the difference (CAM2 - ARM) going to zero around 300mb, unlike the June/July case where the difference maximized at 250mb (Fig. 1). During the 24-hour forecast the ARM shows drying throughout the column (dashed curves) while CAM2 moistens throughout the column except between 700mb and 800mb (solid curves). Thus, after 24 hours the CAM2 is too moist throughout most of the column, unlike the June/July case where it was too dry below 500mb (Fig. 1).

Fig. 6 shows the vertical profiles of the 24-hour average of terms in the specific humidity forecast equation (1) for the composite CAM2 forecast and corresponding ARM data. In contrast to the June/July case shown in Fig. 2, the CAM2 total tendency (solid blue) is near zero except below 900mb where it is positive (Fig. 6a). The ARM total ten-

dency (dashed blue) is slightly negative throughout the column, but small compared to the advection and parameterization terms. This is consistent with the precipitable water increasing in CAM2 and decreasing in ARM that was seen above in Fig. 4d.

Fig. 6a shows that compared to ARM the CAM2 advection (red curves) is somewhat stronger than the ARM below 700mb and somewhat weaker above. The overall impression is that the CAM2 advection, while similar to ARM, occurs slightly lower in the troposphere. This structure is mirrored in the vertical advection (Fig. 6c, green curves). Notice that CAM2 captures the small region of negative vertical advection centered on 900mb. The horizontal advection in CAM2 (solid blue) dries the column above 700mb and moistens it below. Overall the structure of the CAM2 horizontal advection is similar to that of ARM but the amplitude is somewhat larger, being more negative above 700mb and more positive below. Except in the lowest layers, the parameterizations (solid green) balance the advection in CAM2 (Fig. 6a) leading to the small total tendency in CAM2. In ARM, the parameterizations (dashed green) are slightly larger in magnitude than the advection, leading to a drying of the column. Thus the parameterizations appear to be a little weak in CAM2. Near the surface, CAM2 parameterizations moisten, while the ARM data indicate drying. This follows from the CAM2 latent heat flux being larger than that of ARM, to be discussed below.

The CAM2 and ARM parameterizations match as closely as they do in Fig. 6a because of our decision to average the single grid points where the CAM2 precipitation matched that of ARM. For the four grid point average, the CAM2 parameterization and

advection curves have the same shape as those in Fig. 6a, but the amplitude is reduced to about two-thirds the value, which is consistent with the precipitation ratio. A similar reduction in amplitude occurs with the terms in the temperature equation to be discussed below.

Fig. 6b shows the components of the parameterized processes for CAM2. The moist processes (red) are dominant above 900mb and thus apparently do not remove enough moisture compared to ARM. The PBL parameterization (blue) moistens too much near the surface, presumably in response to the CAM2 latent heat flux being larger than ARM by about 30W/m<sup>2</sup> (Table 2). However, Boyle et al. (2004) find that the land is too dry in the initial conditions. This finding coupled with the observation that the CAM2 becomes too moist seems inconsistent with a too large latent heat flux in CAM2. As in the July case, this moisture inconsistency and the temperature - sensible heat flux situation discussed below implies that the exchange parameterization formulation should be examined further. The prognostic cloud water parameterization (Fig. 6d, yellow curve) dominates the total moist processes (red curve) below 800mb and the Hack convective parameterization (green curve) dominates above 800mb. The Zhang-McFarlane convective parameterization (blue) contributes very little. The three forms of rainfall evaporation are also small.

Fig. 7 shows vertical profiles of the terms in the thermodynamic equation

$$\frac{\partial T}{\partial t} = -\mathbf{V} \cdot \nabla T - \dot{\sigma} \frac{\partial T}{\partial \sigma} + \kappa T \frac{\omega}{p} + Q \quad (2)$$

where the heating term  $Q$  consists of the sub-grid scale parameterizations, which we sepa-

rate into three primary components: radiation, moist processes and PBL, the latter two as in the humidity equation. The term  $\kappa T\omega/p$  in (2) is referred to as the energy conversion term.

As seen in Fig. 7a, the dynamical tendency, which is the sum of the first three terms on the right-hand-side of (2), is weaker in CAM2 than in ARM above 800mb (red curves), i.e. CAM2 cools less than ARM. To a large extent this occurs because the energy conversion term is weaker in CAM2 (Fig. 7c, yellow curves). This, in turn, is consistent with the CAM2 parameterizations producing less condensed water and thus having a smaller release of latent heat to drive the vertical motion, leading to a weaker pressure vertical velocity ( $\omega$ ) (Fig. 7d). The diabatic heating balances the dynamical cooling to a large extent above 800mb in CAM2 (Fig. 7a, solid curves). As was the case with moisture, in ARM the estimates of the parameterization terms are a little stronger than the dynamics there leading to a cooling (dashed curves). Below 850mb, the CAM2 does not capture the parameterization cooling seen in ARM (Fig. 7a, green curves) even though the ARM sensible heat flux is positive, while that of CAM2 is negative.

In considering the components of the total parameterization tendency in CAM2 (Fig. 7b) the moist processes (red) appear to be responsible for the tropospheric warming, and thus appear to be not acting deep enough. This is consistent with the moist processes not removing enough moisture. The partition of the moist processes into components (not shown) is basically the same as seen in the terms of the moisture equation (Fig. 6d). The prognostic cloud water parameterization dominates in the lower troposphere below 750mb

and the Hack convection parameterization dominates above 750mb in the mid to upper troposphere. Thus the Hack parameterization might not be working deep enough. The Hack parameterization is not a deep penetrative convection scheme. Xie et al. (2002) show that the Hack parameterization in the CCM2 single column model puts the maximum heating rate too low.

Returning to the parameterization components in Fig. 7b, the PBL parameterization (blue) heats at the first model level and cools slightly above. The integral is negative since the CAM2 surface sensible heat flux is negative, but the ARM sensible heat flux is positive (Table 2). The CAM2 atmosphere is warmer at the surface than ARM which could lead to the different sign of heat flux. However the sensible heat flux also depends on the land temperature and Boyle et al. (2004) conclude that the land temperature is too warm in CAM2 in the initial data sets. The cooling by the PBL parameterization is not enough to compensate the warming from the prognostic cloud parameterization, yielding a net a heating near the surface in CAM2 compared to cooling in ARM (Fig. 7a, green curves). Note that the radiation (yellow) is insignificant compared to the other terms throughout the lower troposphere (Fig. 7b).

The insufficient cooling below 850mb in the CAM2 parameterization (fig. 8a, green lines) might arise because CAM2 parameterizations are not re-evaporating enough rain in the surface layers, and/or because of insufficient downdrafts since the Hack scheme does not include that process. The re-evaporation parameterization in CAM2 depends on relative humidity. From the surface to 900mb, where the cooling occurs, the CAM2

relative humidity is the same as that of ARM (not shown). Thus a difference in relative humidity between CAM2 and ARM is not the cause of less re-evaporation in CAM2, if in fact that is the case, and the formulation of the parameterization itself might be deficient. We do note however that if the CAM2 evaporation of rainfall was larger, the parameterized moisture term would be more positive than that seen above in Fig. 6a, and it is already too large compared to ARM. But as also already mentioned, that CAM2 positive value is likely due to the surface evaporation being too large.

Table 2 shows that the CAM2 net radiation is less than both the ARM Variational and the Siros estimates. Thus the net radiation itself is not driving the sum of latent and sensible heat flux in CAM2 to be larger than in ARM by about  $7 \text{ W/m}^2$ . The different balance at the surface must be affecting the CLM2 temperature. The CAM2 net longwave radiation at the surface is greater than in ARM, reflecting a warmer surface in CAM2 (Table 2).

Table 2 shows that the CAM2 significantly overestimates the low and middle level cloud fractions, and the high cloud fraction to some extent. The CAM2 cloud liquid water is also significantly larger than that of ARM (and note that these April values are an order of magnitude larger than the July values shown in Table 1), yet the CAM2 net solar radiation at the surface is only slightly less than that of ARM. This seeming inconsistency is not explainable by the diurnal cycle, as was the inconsistency in June/July. The CAM2 cloud liquid water is significantly larger than that of ARM throughout the entire diurnal cycle. Similarly, the low and mid-level cloud fractions are significantly larger than those

of ARM throughout the entire diurnal cycle. This inconsistency requires further study.

For these precipitation days in April 1997 the differences in the budget terms between the CAM2 and ARM are more subtle than was seen in June/July 1997. Erroneous terms are less blatant than in the June/July 1997 case, and thus probably harder to pursue. Nevertheless, it might be fruitful to examine the Hack convection further with regards to the depth of its activity. As before, that particular component might not be wrong. It might be responding to other erroneous or missing processes.

**Composite light and no rain case.** Fig. 8 shows the evolution of the temperature field for the composite CAM2 forecasts (solid) and ARM (dashed) for days 0, 0.5 and 1. Fig. 8a shows the profiles with a standard atmosphere (Hess, 1959, pps 84-85) removed to enlarge the scale and better show the magnitude of the differences. Fig. 8b shows the actual temperature profiles to make the existence of an inversion at 12Z (06LST) clear. (Recall, the forecasts were initialized at 00Z or 18LST.) Because in this composite the parameterizations have a strong diurnal signal, we include the 12-hour forecast values to isolate differences which develop at nighttime and at daytime, and to eliminate the significant cancellation that occurs in the 24-hour average. (Such cancellation was less of a problem for the balances considered earlier.) After 12 hours, the CAM2 temperature has only a small error (difference of yellow curves in Fig. 8) in the mid-troposphere, 800mb to 250mb. In fact the difference with ARM actually decreases with time from the initial error (difference of blue curves). Thus we consider the CAM2-ARM difference in that region to be within the uncertainty of the atmospheric estimates and consider only the

lower troposphere in the following.

The major temperature error in CAM2 forms below 800mb, where after one day CAM2 becomes too warm by late afternoon at  $t = 1$  (00Z, or 18LST, red curves in Fig. 8). The CAM2 is also too warm in early morning at  $t = 0.5$  (12Z or 06LST, yellow curves), however the difference is comparable in magnitude to the initial difference (blue curves). More noticeable is the temperature gradient below 800mb at  $t = 0.5$  (12Z or 06LST). The CAM2 forms too strong an inversion just above the surface. The first model level is too cold and the levels above retain the initial warm bias.

In parallel with the 12-hour sampling above, we consider 12-hour averages rather than 24-hour averages for the terms in the prediction equations. Fig. 9a shows that the change in temperature from 00Z–12Z is driven mostly by the dynamics (red curves) at the bottom two model levels where the CAM2 cools and the ARM data indicate warming. The parameterized processes (green curves) agree quite well between ARM and CAM2 for the first 12 hours of the forecasts. Fig. 9c shows that below 850mb the dynamics difference is dominated by the horizontal advection (blue curves) with a small contribution by the energy conversion term (yellow curves). In the second 12 hours of the forecast (12Z–24Z) Fig. 9b shows that the CAM2 dynamics continue to cool near the surface while the ARM data continue to indicate warming (red curves). However the parameterizations (green curves) show a much larger difference, with CAM2 warming at almost twice the rate indicated by the ARM data. The PBL parameterization is the dominant component of the total parameterization tendency (not shown) reaching a maximum heating of 9

K/day at the first model level, while the radiation cools at around 1 K/day and the moist processes are even smaller.

Table 3 shows that for the 12Z–24Z period while the CAM2 latent heat flux agrees well with the ARM estimates, the sensible heat flux in CAM2 is  $30 \text{ W/m}^2$  greater than that of ARM. This difference contributes to the PBL parameterization in CAM2 warming more than ARM does in the lower model levels seen in Fig. 9b. We note that Boyle et al. (2004) found the land to be too dry during this period, so it is surprising that the latent heat flux agrees well with ARM. On the other hand, they found that the land was also too warm which could explain the too large sensible heat flux in CAM2.

Concerning the upper troposphere, where the CAM2 forecast temperature difference with ARM was within the uncertainty of the atmospheric estimates, we note that although the total dynamical tendency in the upper troposphere is similar in CAM2 and ARM, the individual components of the tendency are very different (Fig. 9c and d). For both time periods (i.e. 00Z–12Z and 12Z–24Z) the cooling by horizontal advection (solid blue) is a dominant term in CAM2 but rather unimportant in ARM. For the period 12Z–24Z the horizontal advection is balanced by warming from the energy conversion term in CAM2 (solid yellow). The energy conversion term in the ARM data (dashed yellow) is half the strength of that in CAM2 and is balanced primarily by the vertical advection (dashed green) with some contribution from the horizontal advection (dashed blue). For the period 00Z–12Z the energy conversion term (yellow) is similar in ARM and CAM2, but it is balanced primarily by vertical advection in ARM (dashed green) and by horizontal ad-

vection in CAM2 (solid blue). Obviously, the dynamical component of CAM2 requires further investigation in this case even though the net effect on the forecast temperature error is minimal.

Figure 10 shows that the CAM2 becomes too dry in the surface layers after one day (red curves). During the first 12 hours of the forecast, CAM2 and ARM moisten slightly near the surface, while the different vertical gradients seen initially are maintained (yellow curves). During the second 12 hours (ending 00Z, 18LST) the CAM2 does not moisten enough at the surface even though the latent heat fluxes are similar (Table 3) and the vertical gradient becomes noticeably less than that of ARM. Figure 11a shows the partition of the moisture tendency between advection and parameterization for the period 12Z–24Z. The CAM2 parameterizations do not moisten enough near the surface and deposit too much moisture higher in the atmosphere around 750mb (green curves). The CAM2 parameterized moisture tendency is rather uniform up to 700m while in ARM it decreases from the surface to 700mb (green curve, Fig. 11a). In CAM2, the PBL parameterization dominates the total (Fig. 11b), and provides uniform moistening within the boundary layer as reflected in the parameterized moistening (green curve). Boyle et al. (2004) show that for the dry period period, the CAM2 PBL depth is close to observed. The comparison with ARM of the tendencies produced by the parameterization suite seems to imply that the moisture is mixed too uniformly in CAM2. Below 700mb the moist processes tendency is negative but small, countering the PBL moistening only slightly. The moist processes are dominated by drying by the Zhang-McFarlane convection and

moistening by the rainfall evaporation of the Zhang-McFarlane condensate (not shown). But this only occurs on the two days of the averaging period with light precipitation (Fig. 4a). The other days the moist processes have negligible tendencies. Thus since for most of the averaging period the moist processes are inactive, the error in CAM2 is probably a result of the PBL parameterization. However, as mentioned with other situations, that particular component might not be formulated incorrectly. It might be responding to other erroneous processes. Nevertheless, it would be fruitful to examine the PBL parameterization further with regards to its vertical structure.

#### 4. Conclusions

We have considered the balance of terms in the moisture and temperature prediction equations at the ARM SGP site for a series of forecasts with the CAM2. The initial atmospheric conditions are obtained by interpolating high resolution NWP analyses to the coarse resolution climate model grid in a way that is consistent with the low resolution topography, and leads to smooth, balanced forecasts. The land initial conditions are obtained by a spinup procedure in which the CLM2 responds to and interacts with the CAM2 while the CAM2 is forced with NWP analyses to evolve like the observed atmosphere. The land model initialization seems adequate for the experiments reported here because the first-order CAM2 errors are relatively large and presumably not dominated by the surface fluxes. Nevertheless, improvement to the land initialization will be needed in the future as these dominant CAM2 errors are reduced.

The forecasts were for two ARM IOPs, June/July 1997 and April 1997. Composites

of forecasts with like properties were compared to the ARM variational dataset. We use the term “error” to refer to CAM2 minus ARM differences, and imply that this is the model error. One should keep in mind, however, that this difference includes the CAM2 error itself, which we assume to be the dominant component, and errors in the ARM measurements and variational analysis, as well as differences due to the CAM2 and ARM data representing different areas. Some of our errors may be small enough that this assumption is not valid. Unfortunately, it is almost impossible to differentiate between all these sources of differences, especially as error bars for the ARM data are not known.

Budget comparisons as discussed here do not tell us definitively what is wrong with the model. They do, however, indicate which processes are behaving differently in the model from the atmosphere. This does not imply that those processes are formulated in error since they may be responding to errors in other processes. The comparisons do, however, provide an indication of where to begin looking to determine why certain model processes work differently from the observed behavior. Such examinations should provide insight into the workings of the model and ideally lead to suggestions for improvements.

In the cases we consider here, a predominant error generally forms within 24 hours. In some cases the error at day 1 is large enough that examination of the forecast for later elapsed times is not warranted since the model state is too far from the observed atmosphere state and so the parameterizations are no longer operating on the correct state. Thus we limit our analysis to the first 24 hours of the forecasts.

We consider three cases: (1) the June/July 1997 IOP when the atmosphere is rela-

tively moist with precipitable water around 37mm during which the ARM data indicate surface evaporation corresponds to 90% of the precipitation with advection accounting for the remainder; (2) the rainy days of the April 1997 IOP when the atmosphere is less moist with precipitable water around 22mm during which the ARM data indicate that horizontal advection accounts for much of the precipitation with a small contribution from surface evaporation and the balance being derived from the water already present in the column, and (3) light and non rainy days of the April 1997 IOP when the moist process parameterizations are very weak or inactive and the PBL parameterization is dominant. The behavior of the parameterizations in each case is different.

In the June/July 1997 forecasts, when the atmosphere is relatively moist and the dynamical forcing is small, the CAM2 rains most of the time and does not mimic the observed episodic characteristics of the observed rain. The precipitation is entirely convective. In addition, the CAM2 does not maintain observed precipitable water. Based on examining the terms in the moisture prediction equation, it appears that the Zhang-McFarlane convective parameterization drives the model to the wrong state. Within 24 hours, the CAM2 becomes too moist above 500mb and in the surface layers, too dry between 900mb and 500mb, too warm between 900mb and 200mb, and too cold above and below these levels. Of course this does not necessarily imply that the Zhang-McFarlane convection parameterization itself is incorrect. It might be responding to incorrect forcing from some other term such as the PBL parameterization or even the radiation in the thermodynamic equation. Nevertheless, it is a likely candidate deserving further examination, both in its

triggering functions which are being considered, for example, by Xie et al. (2004), and in the state produced by the convection parameterization when it is activated.

Comparison of the CAM2 and ARM surface sensible and latent heat fluxes, the initial land surface conditions, and the net surface radiative fluxes lead to inconsistencies which indicate that the exchange parameterizations should be examined further.

In the April 1997 forecasts, when the atmosphere is less moist and the dynamical forcing is important, the CAM2 captures the episodic nature of the precipitation events very well. Of the total precipitation, the prognostic cloud water parameterization provides one-third of the total and the Hack convective parameterization provides two-thirds.

For the April composite case of rain days, the differences in the budget terms between the CAM2 and ARM are more subtle than was seen in June/July. Overall, the Hack convective parameterization appears to be not acting deep enough. At the same time, and possibly as a consequence, the dynamical component is a little weak. In particular the maximum vertical velocity is too weak and occurs too low in the atmosphere resulting in the energy conversion term being too weak. Of course, the vertical motion is intimately related to the parameterized heating from the release of latent heat, and cause and effect is by no means clear. Nevertheless, it might be fruitful to try to determine why the Hack convective parameterization does not seem to work deep enough. The CAM2 parameterizations also do not cool enough in the lower model levels. This leads us to speculate that the parameterizations do not re-evaporate enough precipitation or that cooling by convective downdrafts is insufficient.

As in the June/July forecasts, inconsistencies between CAM2 and ARM surface sensible and latent heat fluxes, land surface conditions, and the net surface radiative fluxes indicate that the exchange parameterizations should be examined further. In addition, CAM2 low and middle level cloud fractions and cloud liquid water are significantly larger than those of ARM. These inconsistencies require further study. In addition, it would be useful to insert a forward model into CAM2 to directly calculate the variable measured by the satellite for cloud fraction.

For the April composite case over days with light or no rain, the CAM2 has very small temperature error from 700mb to 250mb. Similarly the specific humidity error is relatively small above 700mb. Below 700mb the PBL parameterization is dominant during the daytime. It does not appear to create the correct vertical structure in either temperature or moisture. Thus the PBL parameterization warrants further consideration in these cases. Concerning the upper troposphere where the CAM2 forecast temperature difference with ARM was within the uncertainty of the atmospheric estimates, the total dynamical tendency is similar in CAM2 and ARM. However, the individual components of the tendency are very different between CAM2 and ARM. Thus the dynamical component of CAM2 requires further investigation even though in this case the net effect on the forecast temperature error is minimal.

## ACKNOWLEDGMENTS

We thank the ECMWF for early access to the ERA40 data which were essential for this study. We also thank Nils Wedi (ECMWF) for explaining some of the intricacies of the interpolation methods used operationally at the ECMWF and James Hack (NCAR) for discussions on details of the CAM2 parameterizations.

The National Center for Atmospheric Research is sponsored by the National Science Foundation. At NCAR this work was partially supported by the Office of Biological and Environmental Research, U. S. Department of Energy, as part of its Climate Change Prediction Program. At LLNL this work was also performed under the auspices of the U. S. Department of Energy (USDOE) Office of Science, Biological and Environmental Research (BER) program by the University of California, Lawrence Livermore National Laboratory under Contract W-7405-Eng-48.

## REFERENCES

- Bonan, G. B., K. W. Oleson, M. Vertenstein and S. Levis, 2002: The land surface climatology of the Community Land Model coupled to the NCAR Community Climate Model, *J. Climate*, **15**, 3123-3149.
- Boyle, J., D. Williamson, R. Cederwall, M. Fiorino, J. Hnilo, J. Olson, T. Phillips, G. Potter and S. Xie, 2004: Diagnosis of CAM2 in NWP configuration, *J. Geophys. Res.*, submitted.
- Hack, J. J., 1994: Parameterization of moist convection in the National Center for Atmospheric Research community climate model (CCM2). *J. Geophys. Res.*, **99**, 5551-5568.
- Hess, S. L., 1959: Introduction to Theoretical Meteorology, Henry Holt and Company, New York, xiv+362 pps.
- Holtlag, A. A. M., and B. A. Boville, 1993: Local versus nonlocal boundary-layer diffusion in a global climate model, *J. Climate*, **6**, 1825-1842.
- Kanamitsu, M., W. Ebisuzaki, J. Woollen, S.-K. Yang, J. J. Hnilo, M. Fiorino, and G. L. Potter, 2002: NCEP-DOE AMIP-II Reanalysis (R-2). *Bull. Amer. Meteor. Soc.*, **83**, 1631-1643.
- Kiehl, J. T. and P. R. Gent, 2004: The community climate system model, version two. *J. Climate*, in press.
- Kiehl, J. T., J. J. Hack, G. B. Bonan, B. A. Boville, D. L. Williamson, and P. J. Rasch, 1998: The National Center for Atmospheric Research Community Climate Model: CCM3. *J. Climate*, **11**, 1131-1149.

- Phillips, T. J., G. L. Potter, D. L. Williamson, R. T. Cederwall, J. S. Boyle, M. Fiorino, J. J. Hnilo, J. G. Olson, S. Xie, and J. J. Yio, 2004: Evaluating Parameterizations in General Circulation Models: Climate Simulation Meets Weather Prediction. *Bull. Amer. Meteor. Soc.*, in press.
- Rasch, P. J. and J. E. Kristjansson, 1998: A comparison of the CCM3 model climate using diagnosed and predicted condensate parameterizations. *J. Climate*, **11**, 1587-1614.
- Roads, J. O., S.-C. Chen, M. Kanamitsu and H. Juang, 1998: Vertical structure of humidity and temperature budget residuals over the Mississippi River basin. *J. Geophys. Res.*, **103**, 3741-3759.
- Simmons, A. J. and J. K. Gibson, 2000: The ERA-40 project plan. ERA-40 Project Report series No. 1, ECMWF, Reading, UK.
- White, P. W. (ed.), 2001: FULL-POS Postprocessing and Interpolation, in IFS Documentation Part VI: Technical and Computational Procedures (CY23R4). European Centre for Medium-Range Forecasts, Reading, UK. Also accessible online at [http://www.ecmwf.int/research/ifsdocs\\_old/TECHNICAL/index.html](http://www.ecmwf.int/research/ifsdocs_old/TECHNICAL/index.html)
- Xie, S. and M. Zhang, 2000: Impact of the convection triggering function on single-column model simulations. *J. Geophys. Res.*, **105**, 14,983-14,996.
- Xie, S., K.-M. Xu, R. T. Cederwall, P. Bechtold, A. D. Del Genio, S. A. Klein, D. G. Cripe, S. J. Ghan, D. Gregory, S. F. Jacobellis, S. K. Krueger, U. Lohmann, J. C. Petch, D. A. Randall, L. D. Roistayn, R. C. J. Somerville, Y. C. Sud, K. Von Salzen, G. K. Walker, A. Wolf, J. J. Yio, G. J. Zhang and M. Zhang, 2002: Intercomparison and evaluation of cumulus parameterizations under summertime midlatitude continental conditions. *Quart. J. Roy. Meteor. Soc.*, **128**, 1095-1135.
- Xie, S. C., M. Zhang, J. S. Boyle, R. T. Cederwall, G. L. Potter and W. Lin, 2004: Impact of a revised convective triggering mechanism on CAM2 model simulations: Results from short-range weather forecasts. *J. Geophys. Res.*, in press.

- Zhang, G. J., and N. A. McFarlane, 1995: Sensitivity of climate simulations to the parameterization of cumulus convection in the Canadian Climate Centre general circulation model. *Atmos. Ocean*, **33**, 407-446.
- Zhang, M. H. and J. L. Lin, 1997: Constrained variational analysis of sounding data based on column-integrated budgets of mass, heat, moisture, and momentum: Approach and application to ARM measurements. *J. Atmos. Sci.*, **54**, 1503-1524.
- Zhang, M. H., J. L. Lin, R. T. Cederwall, J. J. Yio, and S. C. Xie, 2001: Objective analysis of ARM IOP data: Method and sensitivity. *Mon. Wea. Rev.*, **129**, 295-311.

Table 1. Mean forecast 0-24 hour average surface fluxes  
and cloud properties for the JUNE/JULY 1997 IOP

	CAM	ARM
Surface Fluxes ( $\text{W/m}^2$ )		
Latent Heat	151.0	113.6
Sensible Heat	19.7	37.4
Net Radiation	164.0	164.3
Net Radiation (SIROS)		165.7
Net Surface Fluxes ( $\text{W/m}^2$ )		
Solar	215.0	229.2
Longwave	51.1	63.5
Cloud Fraction (percent)		
High	65.8	23.3
Middle	13.9	13.5
Low	27.2	3.2
Cloud Liquid Water ( $\text{gram/m}^2$ )	45.6	29.9

Table 2. Mean forecast 0-24 hour average surface fluxes  
and cloud properties for the rain-day composite of April 1997 IOP

	CAM	ARM
Surface Fluxes ( $\text{W/m}^2$ )		
Latent Heat	58.6	28.6
Sensible Heat	-13.3	9.8
Net Radiation	4.1	15.3
Net Radiation (SIROS)		34.1
Net Surface Fluxes ( $\text{W/m}^2$ )		
Solar	27.2	32.2
Longwave	23.1	-1.9
Cloud Fraction (percent)		
High	76.7	63.0
Middle	76.4	24.8
Low	71.2	4.1
Cloud Liquid Water ( $\text{gram/m}^2$ )	531.9	155.8

Table 3. Mean forecast surface fluxes  
for the non-rain-day composite of April 1997 IOP

	CAM	ARM
0-12 hour average		
Surface Fluxes (W/m <sup>2</sup> )		
Latent Heat	11.7	8.0
Sensible Heat	-26.3	-22.6
Net Radiation	-90.3	-5.6
Net Radiation (SIROS)		-31.8
12-24 hour average		
Surface Fluxes (W/m <sup>2</sup> )		
Latent Heat	117.4	115.5
Sensible Heat	162.5	131.1
Net Radiation	381.1	307.4
Net Radiation (SIROS)		379.1

## FIGURE LEGENDS

- Fig. 1. Mean forecast temperature (a) and specific humidity (b) errors at days 0,1,2,3,4,5 for the June/July 1997 IOP. The “error” at day 0 is difference between the ARM data and the ERA40 analysis interpolated to the CAM2 grid.
- Fig. 2. Mean forecast 0-24 hour average of terms in the specific humidity prediction equation for the June/July 1997 IOP for CAM2 (solid) and ARM (dashed). (a) Total (TOT), advection (ADV) and parameterization (PAR) tendencies. (b) Parameterization (PAR), moist process (MOIST) and PBL parameterization (PBL) tendencies from CAM2. (c) Advection (ADV), horizontal advection (HOR) and vertical advection (VER) tendencies. (d) CAM moist process (MOIST), Zhang-McFarlane convection (ZHANG), Hack convection (HACK) and prognostic cloud parameterization (CLOUD) tendencies (solid) and corresponding rainfall evaporation tendencies (dashed) associated with Zhang-McFarlane convection, Hack convection and prognostic cloud parameterization.
- Fig. 3. (a) 0-24 hour average precipitation of individual CAM2 forecasts (solid) and matching ARM data (dashed) for the June/July 1997 IOP for the periods ending on the day indicated on abscissa. (b) Mean forecast precipitable water at days 0,1,2,3,4,5 for the June/July 1997 IOP and matching ARM data (long dash). CAM2<sub>ERA</sub> (solid) and CAM2<sub>R2</sub> (short dash) denote CAM2 forecasts initialized from ERA40 and NCEP R2 reanalyses respectively.
- Fig. 4. (a) 0-24 hour average precipitation of individual CAM2 forecasts (solid) and matching ARM data (dashed) for the April 1997 IOP for the periods ending on the day indicated on abscissa. (b) Mean forecast precipitable water (solid) at days 0,1,2,3,4,5 for the April 1997 IOP and matching ARM data (dashed). (c) as (a) except day 95, 99, and 102 values replaced by single grid box averages (see text). (d) as (b) except mean of forecasts initialized on days 94, 98, and 101 only.

Fig. 5. Mean forecast temperature (a) and specific humidity (b) at days 0 and 1 for the rain-day composite of April 1997 IOP, CAM (solid) and corresponding ARM data (dashed).

Fig. 6. Mean forecast 0-24 hour average of terms in the specific humidity prediction equation for the rain-day composite of April 1997 IOP for CAM2 (solid) and ARM (dashed). (a) Total (TOT), advection (ADV) and parameterization (PAR) tendencies. (b) Parameterization (PAR), moist process (MOIST) and PBL parameterization (PBL) tendencies from CAM2. (c) Advection (ADV), horizontal advection (HOR) and vertical advection (VER) tendencies. (d) CAM moist process (MOIST), Zhang-McFarlane convection (ZHANG), Hack convection (HACK) and prognostic cloud parameterization (CLOUD) tendencies (solid) and corresponding rainfall evaporation tendencies (dashed) associated with Zhang-McFarlane convection, Hack convection and prognostic cloud parameterization.

Fig. 7. Mean forecast 0-24 hour average of terms in the temperature prediction equation for the rain-day composite of April 1997 IOP for CAM2 (solid) and ARM (dashed). (a) Total (TOT), dynamical (DYN) and parameterization (PAR) tendencies. (b) Parameterization (PAR), moist process (MOIST), PBL parameterization (PBL) and radiation (RAD) tendencies from CAM2. (c) Dynamics (DYN), energy conversion term (E C), horizontal advection (HOR) and vertical advection (VER) tendencies. (d) Pressure vertical velocity.

Fig. 8. Mean forecast temperature at days 0, 0.5 and 1 for the non-rain-day composite of April 1997 IOP, CAM (solid) and corresponding ARM data (dashed). (a) with reference atmosphere removed, (b) complete field.

Fig. 9. Mean forecast 0-12 hour average (a,c) and 12-24 hour average (b,d) of terms in the temperature prediction equation for the non-rain-day composite of April 1997 IOP for CAM2 (solid) and ARM (dashed). (a,b) Total (TOT), dynamical (DYN) and parameterization (PAR) tendencies. (c,d) Dynamical (DYN), energy conversion term (E C), horizontal advection (HOR) and vertical advection (VER) tendencies.

Fig. 10. Mean forecast specific humidity at days 0, 0.5 and 1 for the non-rain-day composite of April 1997 IOP, CAM (solid) and corresponding ARM data (dashed).

Fig. 11. Mean forecast 12-24 hour average of terms in the specific humidity prediction equation for the non-rain-day composite of April 1997 IOP for CAM2 (solid) and ARM (dashed). (a) Total (TOT), advection (ADV) and parameterization (PAR) tendencies. (b) Tendencies from CAM2 due to parameterization (PAR), moist process (MOIST) and PBL parameterization (PBL).

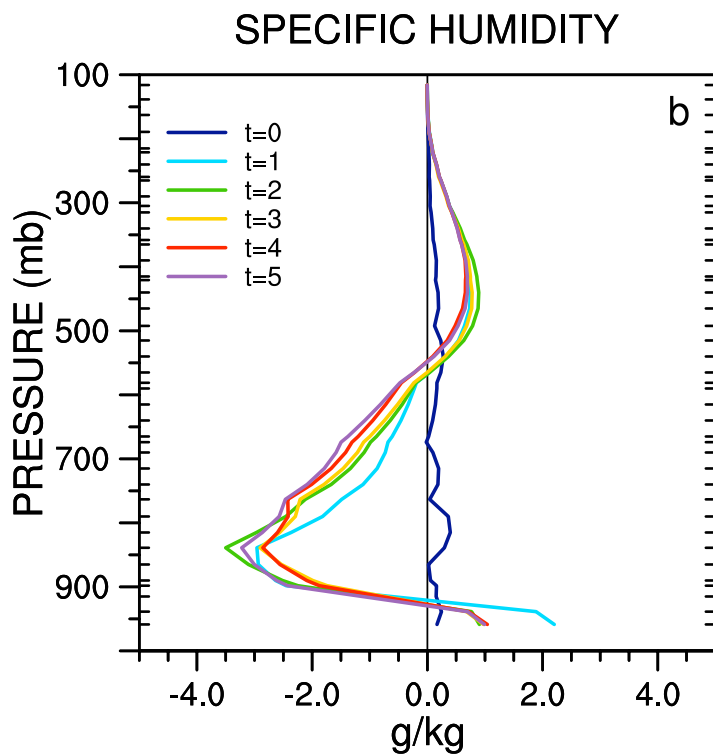
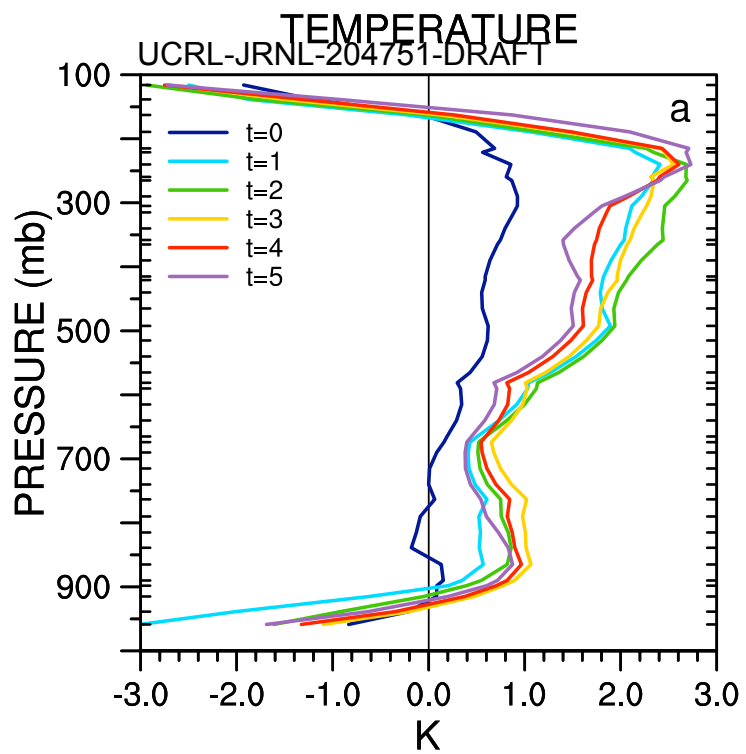


Fig. 1.

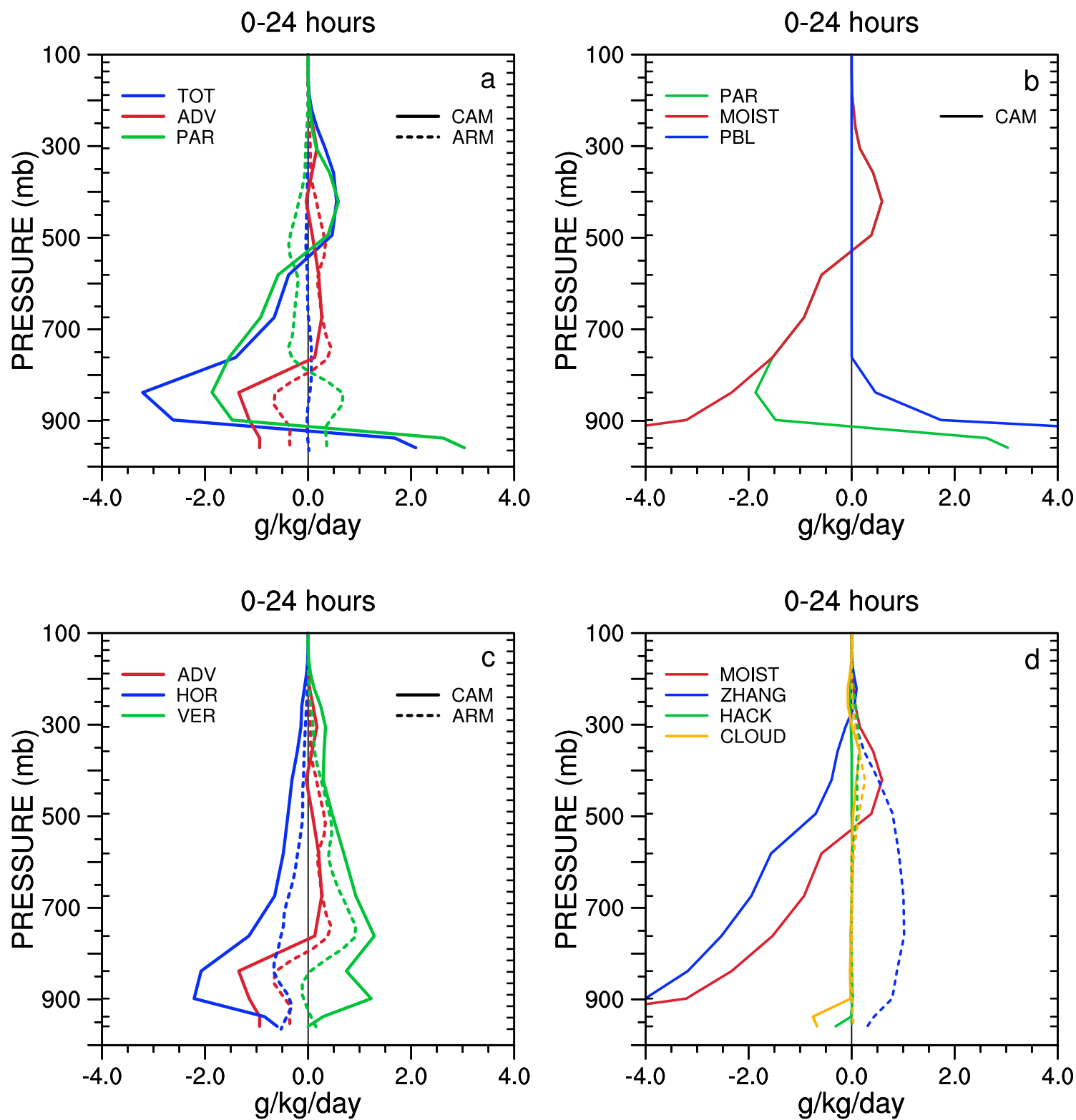


Fig. 2.

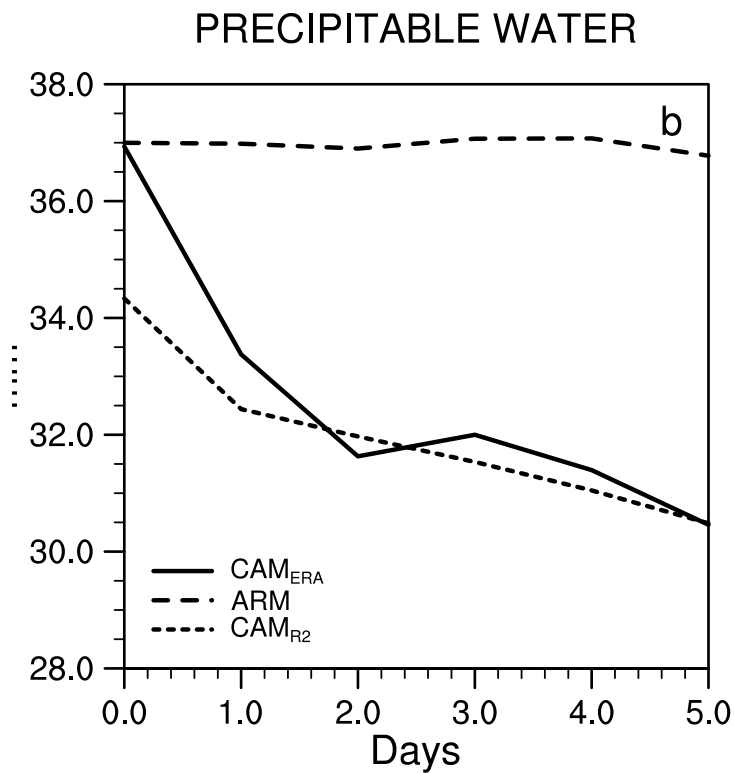
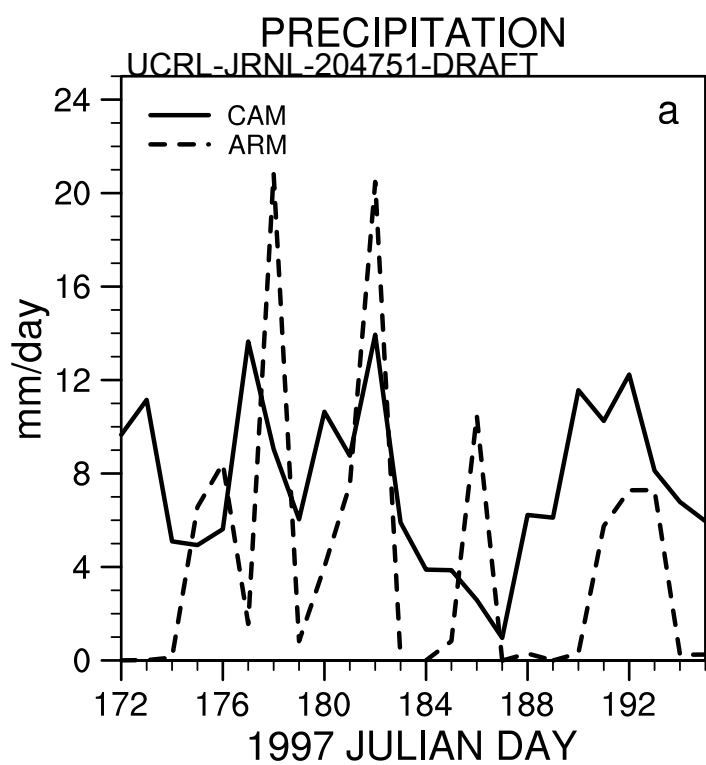


Fig. 3.

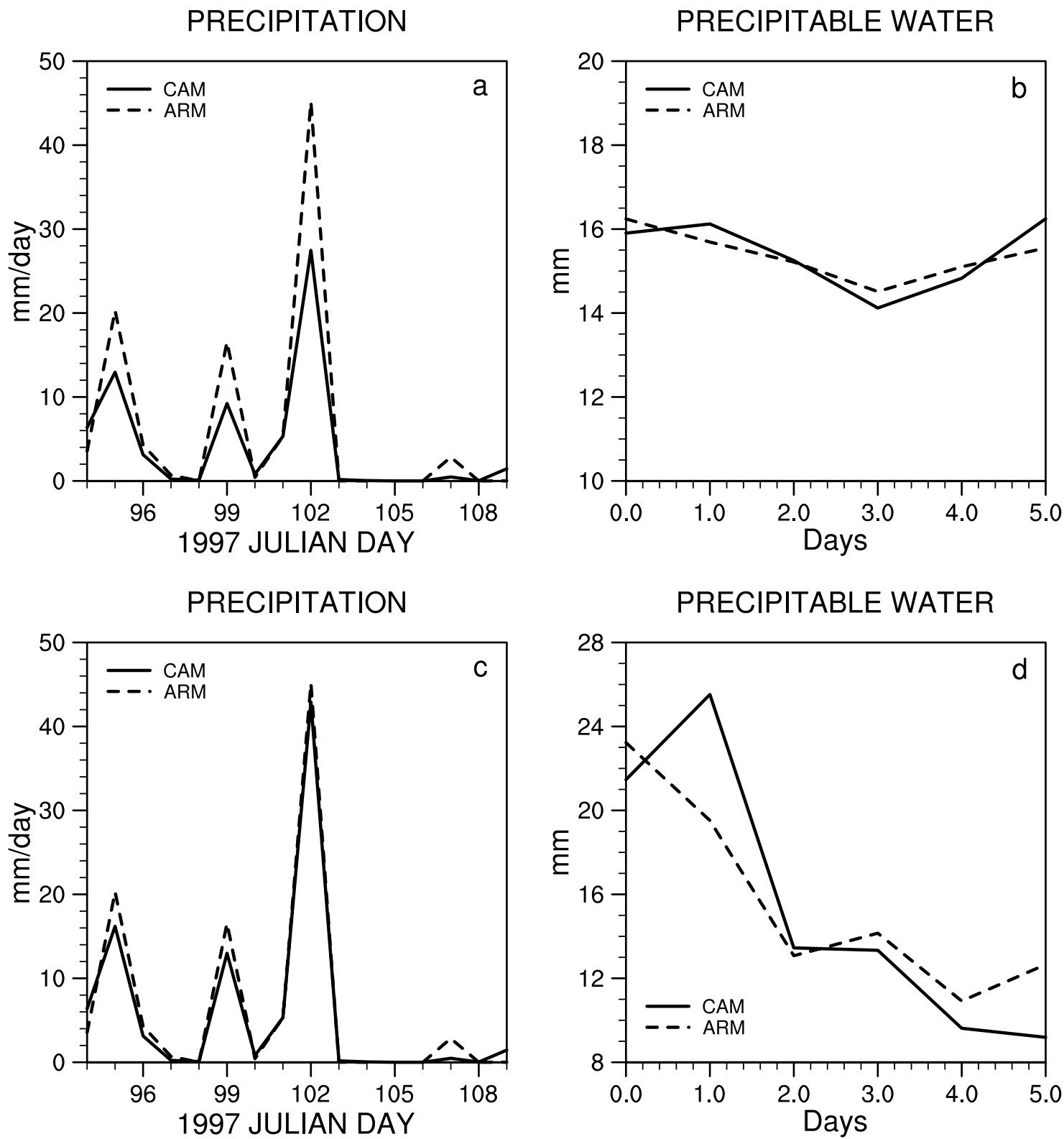


Fig. 4.

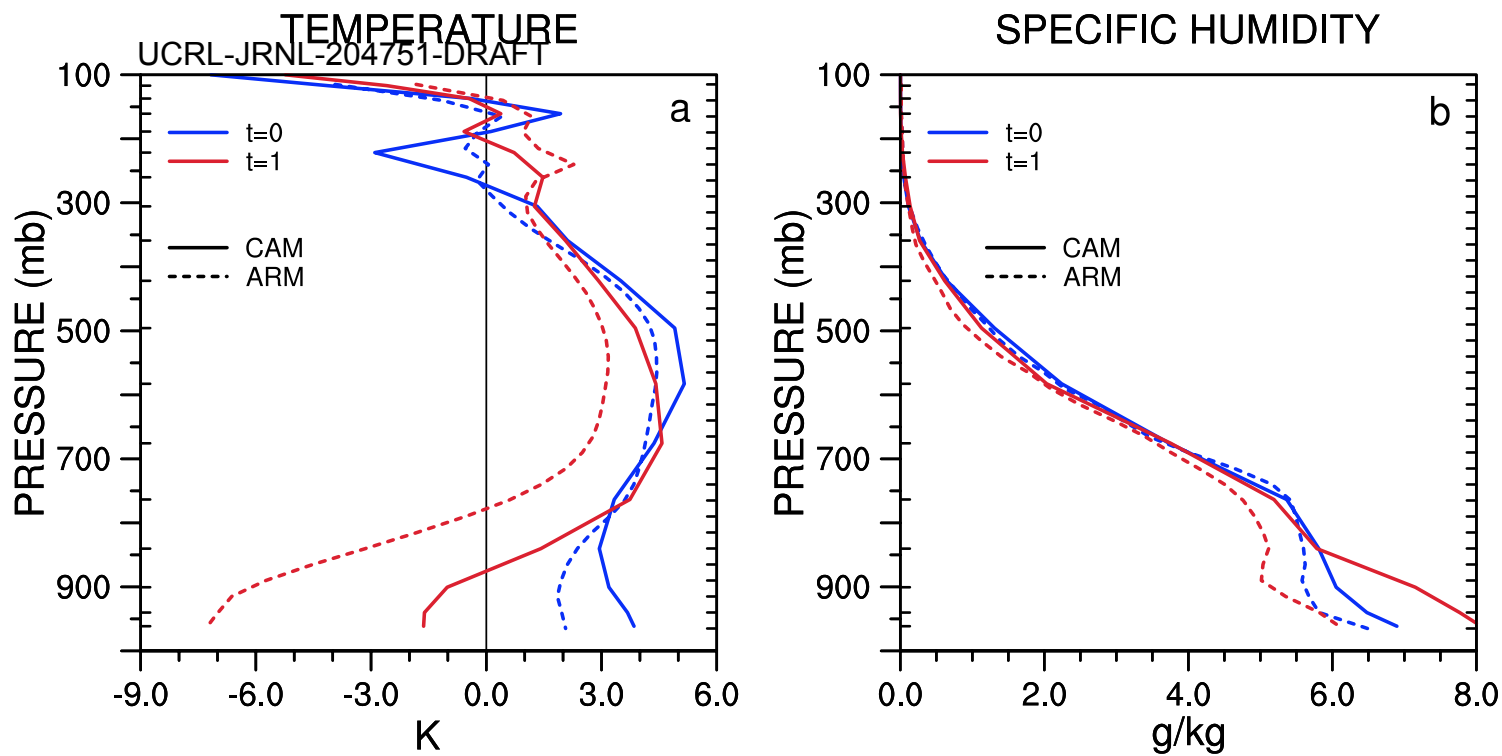


Fig. 5.

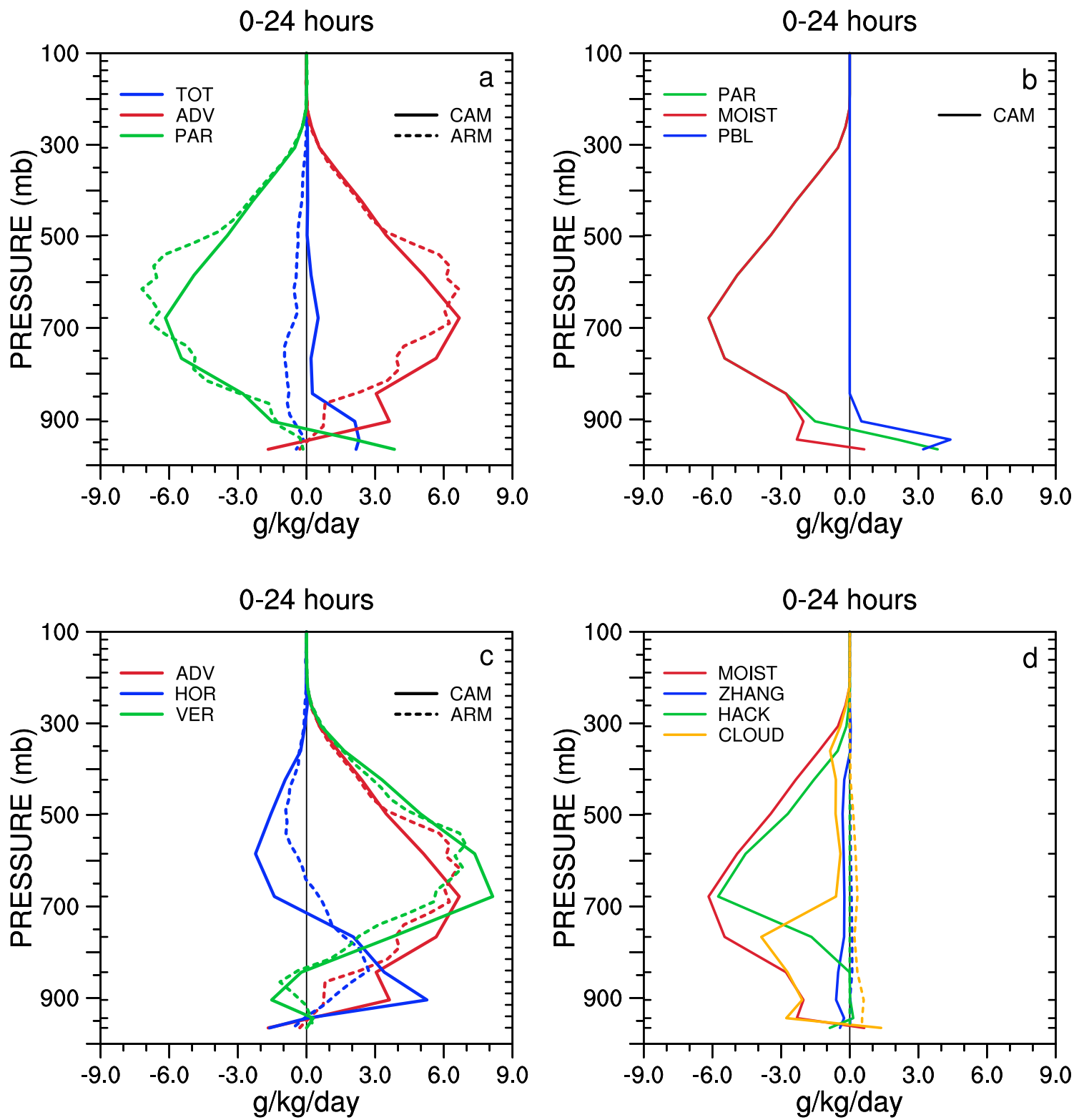


Fig. 6.

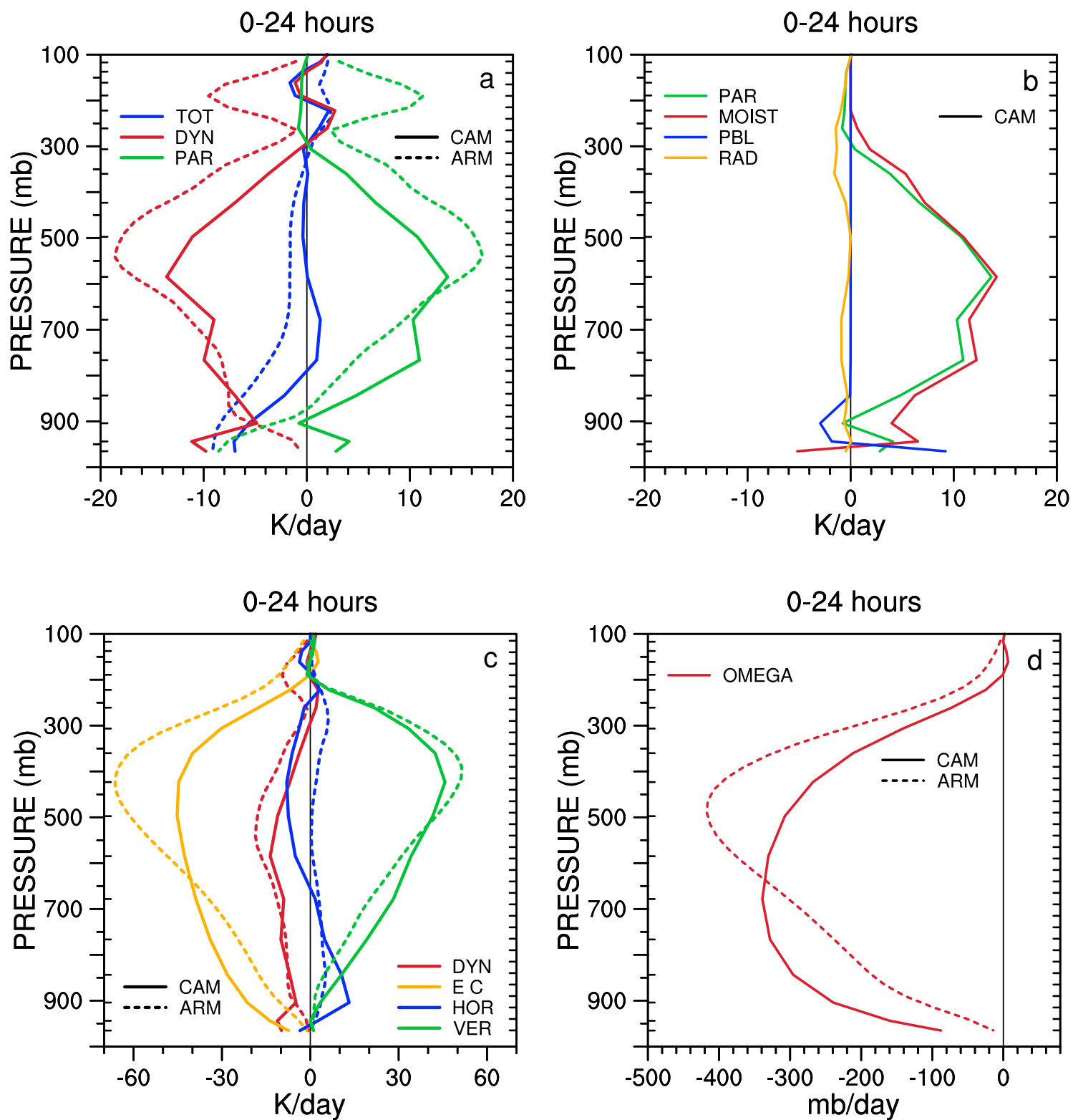


Fig. 7.

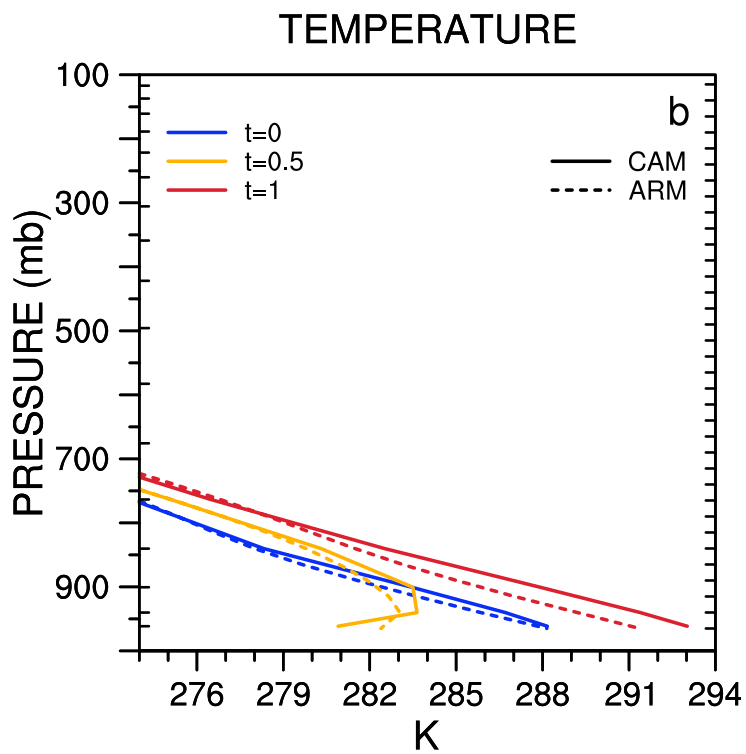
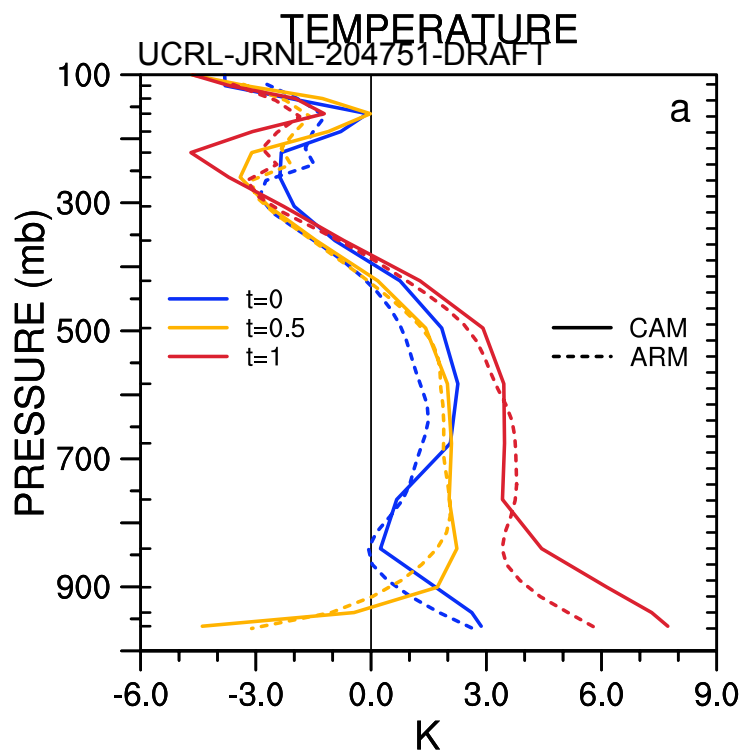


Fig. 8.

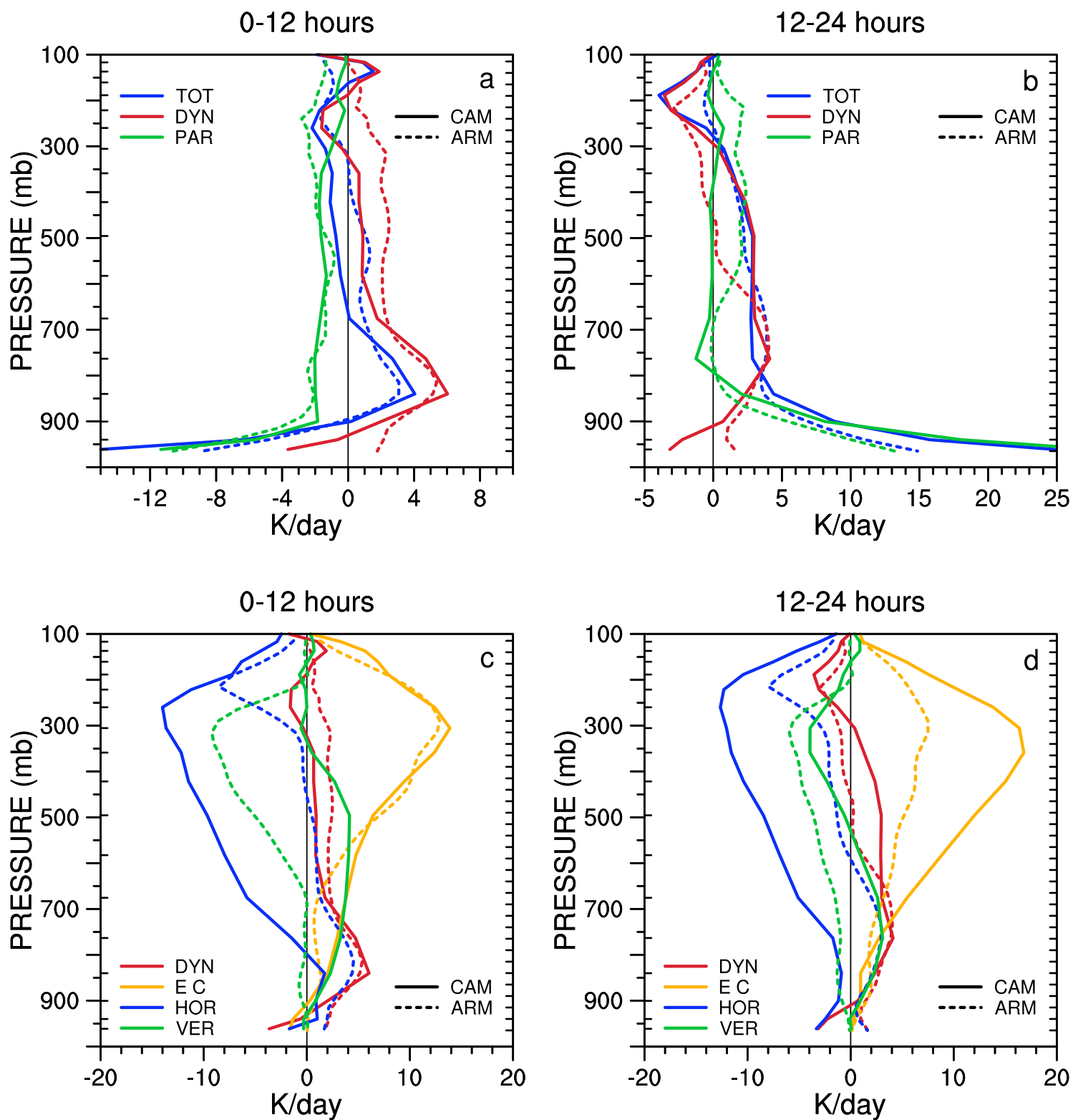


Fig. 9.

## SPECIFIC HUMIDITY

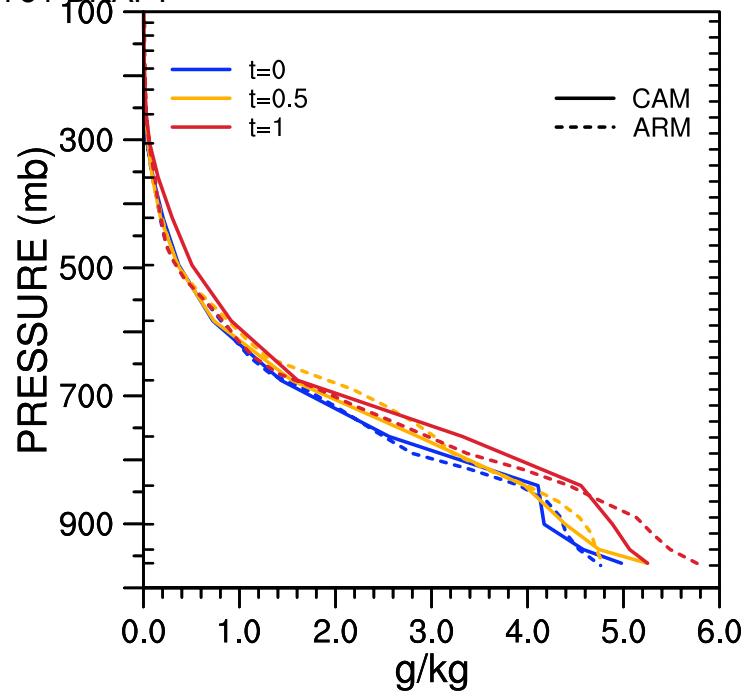


Fig. 10.

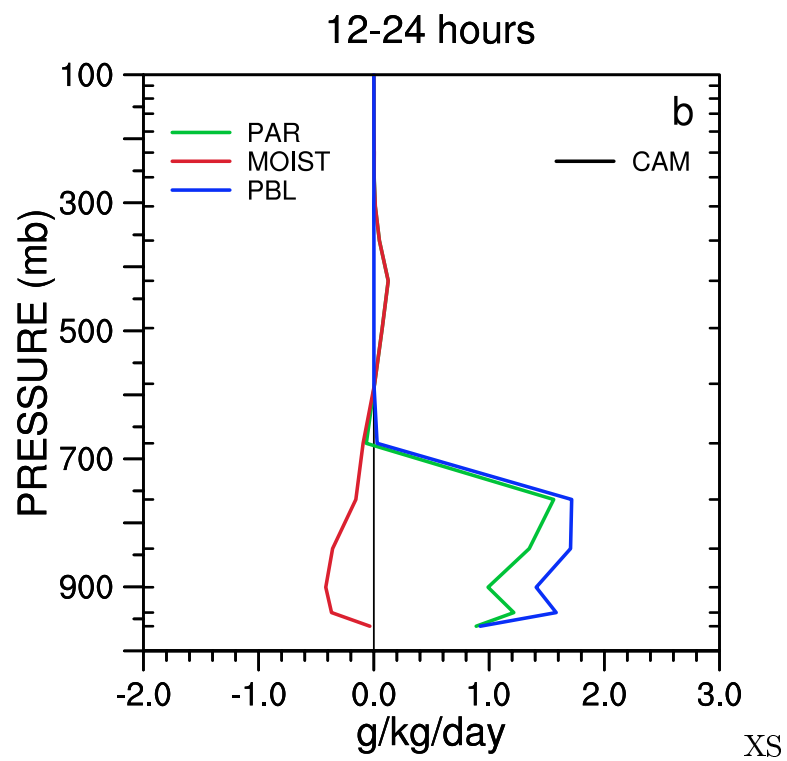
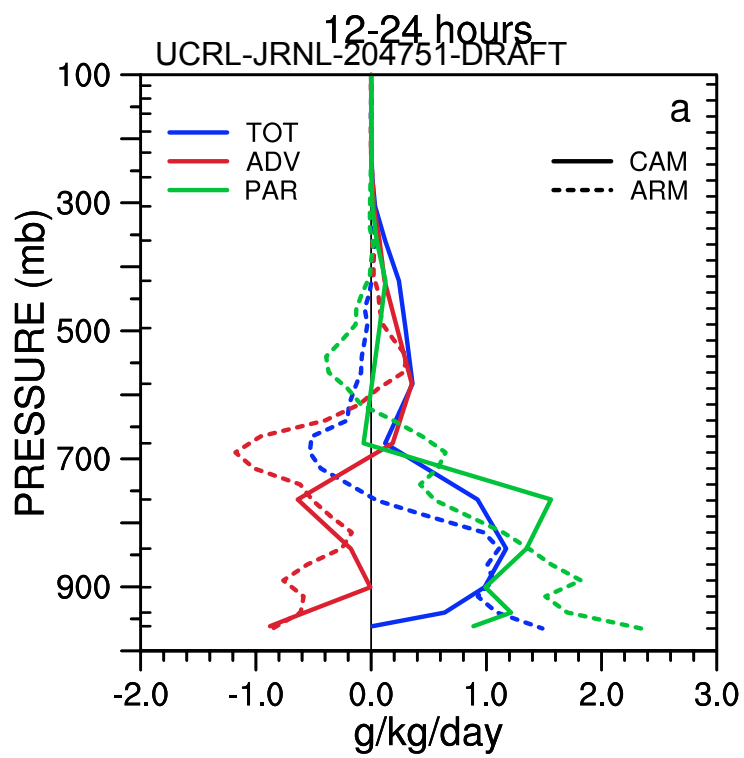


Fig. 11.